J|A|C|S COMMUNICATIONS

Published on Web 07/23/2010

Dynamics of Biocatalytic Microengines Mediated by Variable Friction Control

Samuel Sanchez,*[,†,‡] Alexander A. Solovev,[‡] Yongfeng Mei,[‡,||] and Oliver G. Schmidt[‡,§]

WPI-MANA, National Institute for Materials Science, Tsukuba, Ibaraki, 305-0044, Japan and Institute for Integrative Nanosciences, IFW Dresden, Helmholtzstr 20, D-01069 Dresden, 01069, Germany, Material Systems for Nanoelectronics, Chemnitz University of Technology, Reichenhainer Strasse 70, 09107 Chemnitz, Germany, Department of Materials Science, Fudan University, Shanghai, 200433, Peoples's Republic of China

Received May 30, 2010; E-mail: s.sanchez@ifw-dresden.de

This paper contains enhanced objects available on the Internet at http://pubs.acs.org/jacs.

Abstract: We describe the motion of self-propelled hybrid microengines containing catalase enzyme covalently bound to the cavity of rolled-up microtubes. The high efficiency of these hybrid microengines allows them to move at a very low concentration of peroxide fuel. The dynamics of the catalytic engines is mediated by the generation of front-side bubbles, which increase the drag force and make them turn. The specific modification of the inner layer of microtubes with biomolecules can lead to other configurations to generate motion from different chemical fuels.

Motor proteins powered by chemical fuel have inspired scientists to design hybrid and synthetic nano/micromachines which efficiently generate locomotion (propulsion power) autonomously from their surroundings (chemical).[1] Hybrid machines which couple catalytic biomolecules such as enzymes and artificial nano/microdevices are a promising alternative to the first generation of catalytic nanomotors containing Pt metal as a catalyst toward the finding of higher efficiency conversion, versatile configurations, more physiological conditions, and biocompatible fuels.

Only a few hybrid nanomotors were reported wherein the authors sophistically integrated biomolecules and artificial devices to achieve mechanical energy.[2] More recently, the use of enzymes for locomotion was used by Mano and Heller to propel a carbon fiber (cm scale) at an air−glucose interface.[3] Feringa reported the covalent attachment of enzymes to multiwalled carbon nanotubes (MWCNTs) propelled by a bubble generation,[4] but their trajectory was strongly affected by both the Brownian motion and the position of the enzymes on the MWCNTs. Sen and Mallouk[5] fabricated enzyme−Au/polypyrrole nanords. However, only Brownian motion was observed and no further investigations have been reported so far. Artificial micro- and nanomachines powered by hydrogen peroxide fuel have been intensively investigated and reviewed in recent years.[6] We recently reported the magnetic control over self-propelled rolled-up tubular microengines[7] being used to perform tasks such as the load−transport−delivery of several microobjects.[8] These microengines were propelled by the thrust of oxygen bubbles generated by the catalytical decomposition of H_2O_2 from a Pt film inside the cavity of the microtube.

We report herein the efficient locomotion of biocatalytic microengines by using an enzyme which decomposes peroxide, catalase, and a low concentration of peroxide fuel (1.5 wt %). At this concentration, the hybrid microengines move at 10 body length s^{-1} at the air−water interface compared with 1 body length s^{-1} from the Pt-based microengines.[8] The high efficiency of these microengines is of significant importance toward the design of more powerful nanomachines. This is the first report on the effective use of enzymes as catalysts in self-propelled microengines. Here, we functionalized a thin Au layer with self-assembled monolayers (SAMs) of 3-mercaptopropionic acid (3-MPA) where the enzymes covalently bond. Moreover, as a proof of concept, the specific enzyme binding into the microtubular structures demonstrates that new configurations can be used for autonomous motion toward the finding of more biocompatible fuels.

Scheme 1. (A) Open View of the Hybrid Biocatalytic Microengine; (B) Surface Modification of Inner Au Layer and Enzymatic Decomposition of Peroxide Fuel

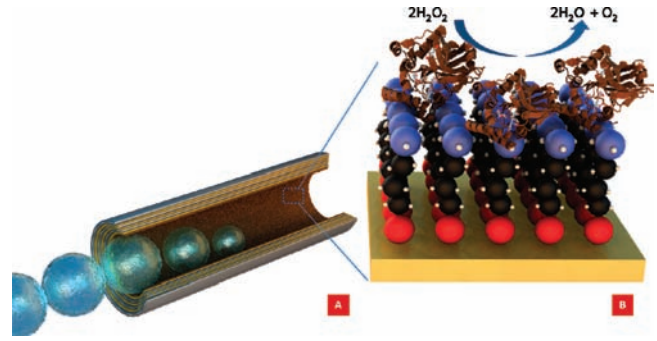

The versatile rolled-up technique allows on-demand fabrication of microtubes by deposition of different materials.[9] We rolled-up thin Ti/Au films into microtubes by selectively under-etching a polymer sacrificial pattern fabricated by photolithography and deposition on Si substrates. Scheme 1A shows an open view of a Ti/Au microtube where the inner Au layer was functionalized with a SAM of 3-MPA (Scheme 1B). The carboxylic terminal groups of the SAMs were converted to amine-reactive esters by the coupling agents 1-ethyl-3-[3-dimethylaminopropyl] carbodiimide hydrochloride (EDC) and *N*-hydroxylsulfosuccinimide (Sulfo-NHS) to covalently bind the protein (i.e., catalase) via carbodiimide reaction. Catalase is one of the most efficient enzymes found in cells since each catalase molecule can decompose millions of hydrogen peroxide molecules every second.[10] The hybrid microtubes (Ti/Au−SAM−catalase) show autonomous motion when immersed in peroxide solution, whereby the enzyme decomposes peroxide into water and molecular oxygen, which, in turn, propels the microengine.

In a typical experiment, Ti/Au rolled up microtubes were incubated into a 20 mM solution of 3-MPA for 45 min. After washing with isopropanol for 5 min, the tubes were immersed in a 1 mL solution which contained the coupling agents EDC (0.05 M) and Sulfo-NHS (0.015 M) and catalase (2 mg mL^{-1}). This incubation was carried out overnight at 37 °C and thereafter rinsed with PBS pH 5.5 and SDS 0.05 wt % for 15 min at each step.

[†] WPI-MANA, National Institute for Materials Science.
[‡] Institute for Integrative Nanosciences, IFW Dresden.
[§] Chemnitz University of Technology.
[||] Fudan University.

10.1021/ja104362r

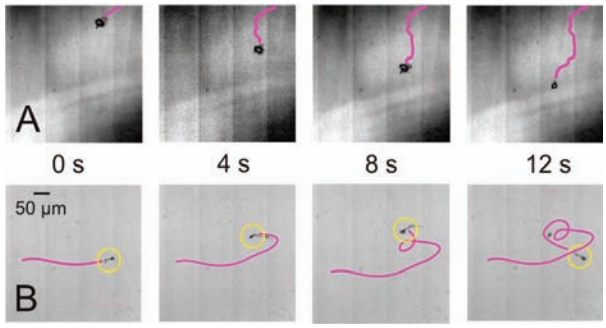

Figure 1. Tracking trajectories of a 25 μm long Ti/Au hybrid microengine with (A) physically adsorbed catalase (B) and thiol−catalase in 1.5% H_2O_2.

In a comparative experiment, the Ti/Au microtubes were incubated overnight at 37 °C with a catalase solution (2 mg mL^{-1}) to physically adsorb the enzyme into the microtube. In a representative example, Figure 1 shows the tracking trajectories of physically adsorbed Ti/Au−catalase (Figure 1A) and covalently modified Ti/Au−SAM−catalase microengines (Figure 1B) during a period of 12 s in 1.5 wt % H_2O_2. A dramatic increase in the mobility of the hybrid microengines was observed for those functionalized with thiol groups (Figure 1B, and videos 1 and 2) where the continuous thrust of bubbles exerts a force which propels the microjet at an average speed of 226.1 ± 21.1 μm s^{-1} for $n = 7$ data points. In contrast, the catalase-adsorbed microengines move at speeds of 40 μm s^{-1} halting shortly after their activation (approximately 1 min.).

Additional control experiments, performed with Ti/Au microtubes under the same fuel conditions resulted in static microtubes (data not shown). Thus, this evidence clearly indicates that the generation of oxygen bubbles into the microtubes arises from the biochemical decomposition of the peroxide by the enzyme catalyst. Contact angle measurements confirmed the gold−thiol bond given that the contact angles changed from 73.3° ± 3.2° to 53.2° ± 1.3° when a volume of 0.75 μL of H_2O was dropt onto Ti/Au and Ti/Au−SAM surfaces respectively ($n = 6$). The samples became even more hydrophilic after incubating the Ti/Au−thiol sample with catalase, denoted by the decrease in the contact angle to 24.3° ± 2.4° ($n = 6$). These results prove the successive functionalization and therefore the coupling of the enzyme to the Au surface.

Interestingly, bubbles forming at the mouth of the microengines, "front-side bubbles," are also observed for the enzyme-modified microengines. The dynamics of the biocatalytic microengines is influenced by the variable viscous drag force exerted by the front-side bubbles which creates a torque and leads to turns and circles.

Figure 2 shows a full rotation of a 25 μm long microjet during a period of 3.5 s while creating and releasing two consecutive front-side bubbles. The bubbles emerged during the first 0.5 s, and they moved to the left side of the microengine. Immediately after, the microtube starts to change its direction and thus rotates counterclockwise (CCW), reducing its velocity. While rotating, the oxygen bubbles are continuously growing, and after 2.5 s, they detach. After being freed from the extra drag force exerted by the bubbles, the microjet experiences a pronounced acceleration (see Figures S1 and S2 in the Supporting Information (SI)). Therefore, the analysis of the motion regarding the size of the front-side bubbles is crucial for understanding the "autonomous" steering of hybrid microjets. Figure S3 plots the quantitative analysis of the angle of rotation and speed with the diameter of the front-side bubble. Briefly, when releasing small front-side bubbles, i.e. 3 μm in diameter, the microengines do not change significantly their direction and likewise their speed is only slightly reduced. This scenario can be reproduced by adding small amounts of common soap to the fuel solution (see Figure S5 in the SI and video 3). In contrast, when these front-side bubbles are larger than the diameter of the microtubes (i.e., from 4 to 12 of diameter) the speed decreases linearly following the Stokes law. The hybrid microengines exhibit a force of 16.44 ± 0.75 pN, which is 5 times higher than the one reported for 50 μm long Pt-based microengines,[8] indicating that large spherical particles could be transported by these novel microengines.

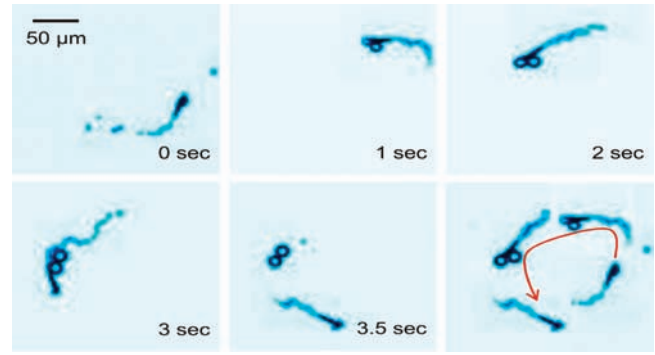

Figure 2. Dynamic steering and full rotation of a Ti/Au−thiol−catalase microengine by the generation of "front-side bubbles".

Similarly, the angle of rotation is reduced inducing a change of direction providing an autonomous steering mechanism (see Figures S3 and S4 in the SI).

In conclusion, we have designed a novel hybrid biocatalytic microengine based on the use of a catalytic enzyme, catalase. This novel approach leads to faster, more powerful, and more efficient microengines compared with those based on a Pt catalyst as well as the use of lower concentrations of peroxide fuel. In doing so, we have demonstrated the ability to functionalize the inner layer of the microtubular engines. These hybrid biocatalytic microengines pave the way to other chemical configurations to induce motion and toward the finding of biocompatible fuels and, why not, to biochemically sense their environment.

Acknowledgment. This work was supported by the WPI Research Center Initiative on MANA, MEXT, Japan and the Grant from the Volkswagen Foundation (I/84 072).

Supporting Information Available: Experimental section, reagents, additional figures and additional discussion. This material is available free of charge via Internet at http://pubs.acs.org.

References

(1) (a) Ozin, G. A.; Manners, I.; Fournier-Bidoz, S.; Arsenault, A. *Adv. Mater.* **2005**, *17*, 3011–3018. (b) van den Heuvel, M. G. L.; Dekker, C. *Science* **2007**, *317*, 333–336. (c) Goel, A.; Vogel, V. *Nat. Nanotechnol.* **2008**, *3*, 465–475. (d) Sen, A.; Ibele, M.; Hong, Y.; Velegol, D. *Faraday Discuss.* **2009**, *143*, 15–27. (e) Wang, J.; Manesh, K. M. *Small* **2010**, *6* (3), 338–345. (f) Mirkovic, T.; Zacharia, N. S.; Scholes, G. D.; Ozin, G. A. *Small* **2010**, *6,2*, 159–167. (g) Ebbens, S. J.; Howse, J. R. *Soft Matter* **2010**, *6*, 726–738.
(2) (a) Skoog, R. K.; Bachand, G. D.; Neves, H. P.; Olkhovets, A. B.; Craighead, H.; Montemagno, C. D. *Science* **2000**, *290*, 1555–1558. (b) Cameron, L. A.; Footer, M. J.; van Oudenaarden, A.; Theriot, J. A. *Proc. Natl. Acad. Sci. U.S.A.* **1999**, *96*, 4908–4913. (c) Weibel, D. B.; Garstecki, P.; Ryan, D.; DiLuzio, W. R.; Mayer, M.; Seto, J. E.; Whitesides, G. M. *Proc. Natl. Acad. Sci. U.S.A.* **2005**, *102*, 11963–11967.
(3) Mano, N.; Heller, A. *J. Am. Chem. Soc.* **2005**, *127*, 11574–11575.
(4) Pantarotto, D.; Browne, W. R.; Feringa, B. L. *Chem. Commun.* **2008**, 1533–1535.
(5) Wang, Y.; Hernandez, R. S.; Bartlett, D. J.; Bingham, J. M.; Kline, T. R.; Sen, A.; Mallouk, T. E. *Langmuir* **2006**, *22*, 10451–10456.
(6) (a) Paxton, W. F.; Sundararajan, S.; Mallouk, T. E.; Sen, A. *Angew. Chem., Int. Ed.* **2006**, *45*, 5420–5429. (b) Mallouk, T. E.; Sen, A. *Sci. Am.* **2009**, *300*, 72–77. (c) Wang, J. *ACS Nano* **2009**, *3*, 4–9. (d) Sanchez, S.; Pumera, M. *Chem.—Asian J.* **2009**, *4*, 1402–1410.
(7) Solovev, A. A.; Mei, Y. F.; Bermúdez-Ureña, E.; Huang, G. S.; Schmidt, O. G. *Small* **2009**, *5*, *14*, 1688–1692.
(8) Solovev, A. A.; Sanchez, S.; Pumera, M.; Mei, Y. F.; Schmidt, O. G. *Adv. Funct. Mater.* **2010**, in press (DOI: 10.1002/adfm.200902376).
(9) (a) Schmidt, O. G.; Eberl, K. *Nature* **2001**, *410*, 168. (b) Mei, Y. F.; Huang, G. S.; Solovev, A. A.; Bermúdez-Ureña, E.; Mönch, I.; Ding, F.; Reindl, T.; Fu, R. K. Y.; Chu, P. K.; Schmidt, O. G. *Adv. Mater.* **2008**, *20*, 4085–4090.
(10) Betancor, L.; Hidalgo, A.; Fernández-Lorente, G.; Mateo, C.; Fernández-Lafuente, R.; Guisan, J. M. *Biotechnol. Prog.* **2003**, *19*, 763–767.

JA104362R